

Effect of Reactor Materials on the Properties of Titanium Oxide Nanotubes

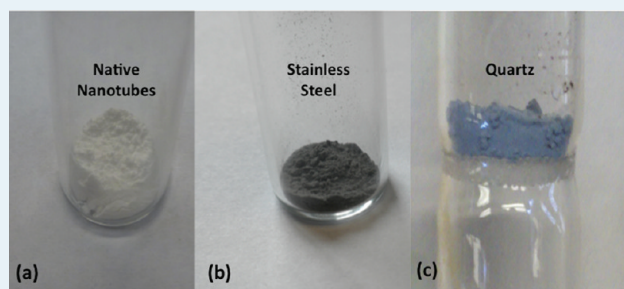
Alon Danon,[†] Kaustava Bhattacharyya,[†] Baiju K. Vijayan,^{†,‡} Junling Lu,[§] Dana J. Sauter,^{†,||} Kimberly A. Gray,[‡] Peter C. Stair,^{†,§} and Eric Weitz[†]

[†]Institute for Catalysis in Energy Processes and Department of Chemistry, [‡]Institute for Catalysis in Energy Processes and Department of Civil and Environmental Engineering, Northwestern University, Evanston, Illinois 60208, United States

[§]Energy System Division, Argonne National Laboratory, Argonne, Illinois 60439, United States

ABSTRACT: Subtleties in the synthesis of materials can have a profound effect on the catalytic and photocatalytic properties of materials. Black TiO₂ nanotubes, demonstrating remarkable solar absorption, were synthesized using a stainless steel reactor. Using UV–vis diffuse reflectance spectroscopy, XPS, EDS, ICP, and TEM, the change in electronic absorption of the TiO₂ nanotubes is explained by the discrete introduction of Cr concentrated particles from the stainless steel reactor. The black TiO₂ nanotubes displayed significant solar-driven photocatalytic activity with the photo-oxidation of acetaldehyde under visible light ($\lambda > 450$ nm).

KEYWORDS: titanium oxide, titania, nanotubes, photocatalysis, chromium



TiO₂ nanotubes in various environments: (a) Native nanotubes (b) Nanotubes in air at RT after H₂ treatment at 350 °C (c) Nanotubes in H₂ at RT after H₂ treatment at 350 °C.

Metal oxide-based nanotubes (NTs) have generated significant scientific interest as a result of their intriguing structure–activity relationship (SAR), which results from their 1D morphologies.¹ Of particular interest are NTs based on titanium oxides in view of the fact that they generally have greater morphological stability than other metal oxide NTs.¹ In addition, titanium oxide NTs exhibit an unusual SAR, which has led to their proposed utilization for a number of applications, including dye-sensitized solar cells,⁴ photocatalysis,^{2,3} sensors,^{5,6} and batteries.⁷ For both sensor and photocatalytic applications, NTs based on titanium oxides share the important common attributes of high surface area, tubular structures, highly active surface sites on the tube walls, and unique morphology.⁶ For sensor applications, titanium oxide-based NTs synthesized by anodizing titanium foil produce a nanotube array architecture that displays remarkable sensitivity toward hydrogen.⁵ These NTs, when exposed to alternating atmospheres of nitrogen containing 1000 ppm of hydrogen and air, can exhibit variations in electrical resistance, at RT, of up to 8.7 orders of magnitude.⁶ This effect has been explained by direct chemisorption of hydrogen on the NTs leading to a tremendous reduction in resistance of the NTs. The activation of hydrogen is proposed to occur on the walls of the undoped nanotubes at highly active surface sites located at nanoscale surface defects.⁶ This result also suggests possible low-energy reactive pathways for the formation of oxygen vacancies with the production of water as the driving force.

The use of titanium oxide-based NTs in photocatalysis has been limited mainly to the UV region, since the electronic

absorption of the native NTs begins at ~ 380 nm.^{2,3} Consequently, for this material, only 2–3% of the solar spectrum can be utilized to drive a photocatalytic reaction. Motivated by a desire to improve the efficiency of solar driven reactions, NTs synthesized by both electrochemical anodization^{8,9} and hydrothermal synthesis^{10,11} techniques have been doped by nitrogen and metals in an attempt to alter the band gap to produce an increase in photon absorption in the visible region of the spectrum.

Recent studies performed on crystalline TiO₂ anatase nanoparticles report that an enhanced solar absorption can be achieved through the introduction of disorder in the surface layers of the nanophase TiO₂ through hydrogenation.¹² It was reported that exposure to hydrogen led to a remarkable change in color, from white to black, as midband gap states are proposed to form with energy distributions that differ from that of a single crystal defect. Remarkably, the change in color was reported to persist for over a year's time. The synthesis of these TiO₂ black anatase nanoparticles involves a high-pressure hydrogen treatment in which the nanoparticles are "hydrogenated" for a significant period of time under relatively harsh conditions: 20.0 bar H₂ atmosphere at approximately 200 °C for 5 days in a stainless steel container.

In this Letter, we report the synthesis and characterization of black titanium oxide NTs and their activity toward acetaldehyde

Received: August 3, 2011

Revised: October 31, 2011

Published: November 01, 2011

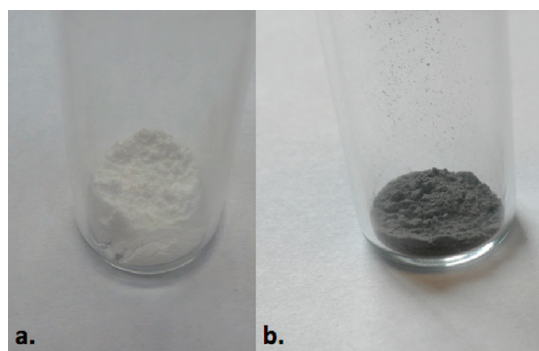


Figure 1. The nanotubes powder (a) before and (b) after being exposed to flowing atmosphere of 5% H_2 in Ar in a stainless steel cell.

oxidation under visible light. As will be discussed below, we observed formation of black NTs, but their formation was dependent on the material of the reaction vessel. With a stainless steel reactor at elevated temperatures and under the flow of hydrogen, the NTs changed color from white to black.¹² However, when the same procedures were implemented in a quartz tube reactor, the color of the nanotubes changed to blue, and on exposure to air, reverted back to their native white color. Hence, subtleties in the choice of reaction conditions not typically expected to affect the properties of materials being synthesized can play a major role in the characteristics of the resulting material. The possible cause of this difference in behavior for our NTs as a function of reactor material will be discussed.

The titanium oxide-based nanotubes were prepared by a modification of a previously reported hydrothermal method.³ Briefly, 2 g of anatase titania powder (assay 99%, Sigma Aldrich Chemicals, USA) was stirred with 50 mL of 10 M NaOH solution (assay 97%, BDH Chemicals, USA) in a 125 mL Teflon cup. The Teflon cup was heated in an oven for 48 h at 120 °C. The resultant precipitate was washed with 1 M HCl (assay 38%, EMD Chemicals, USA), followed by several washings using deionized water to attain a pH between 6 and 7. Nanotubes synthesized via this method are reported to consist of a sheet of titanate, $H_2Ti_3O_7$, which rolls along the [001] direction of the $H_2Ti_3O_7$ structure to produce a folded tubular structure.¹³ The titanate nanotube powder thus formed was dried in an oven at 110 °C overnight.

A DRUV-vis Harrick cell was used for in situ diffuse reflectance UV-vis spectroscopy to measure the change in the electronic absorption spectrum of the materials. $BaSO_4$ was used as a standard. A flow of 5% H_2 in Ar was introduced into the reactor, and the temperature was elevated to 350 °C. The partial reduction of the samples was monitored in situ at both elevated temperatures and after cooling. Figure 1 shows a picture of the titanate NTs before and after being exposed to a flow of 5% H_2 in Ar at atmospheric pressure and 350 °C, for 3 h in a stainless steel Harrick cell. The titanate NTs change color from white to gray/black. Figure 2 compares the diffuse reflectance UV-vis spectra of the titanate NTs before and after this pretreatment. The H_2 -treated titanate NTs display a significant change in the electronic spectrum, leading to effectively complete absorption of light throughout the visible spectrum.

X-ray photoelectron spectroscopy (XPS) measurements were performed on the black NTs and untreated anatase powder used as a precursor for the nanotubes (for comparison) using an Omnicometer Electron Spectroscopy for Chemical Analysis

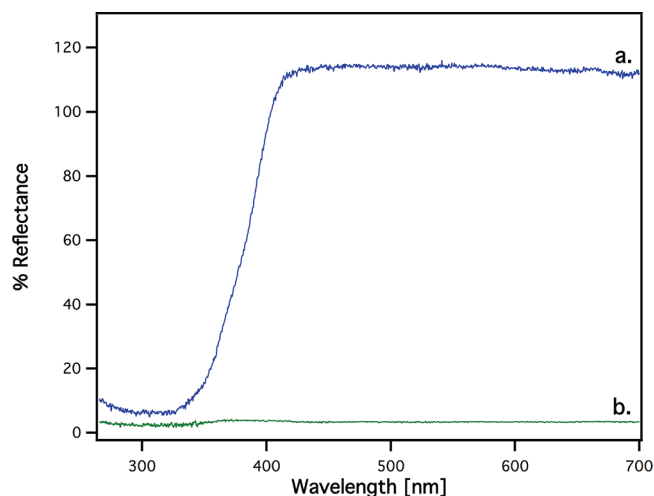


Figure 2. DRUV-vis of the nanotubes powder (a) before and (b) after being exposed to a flowing atmosphere of 5% H_2 in Ar in a stainless steel cell.

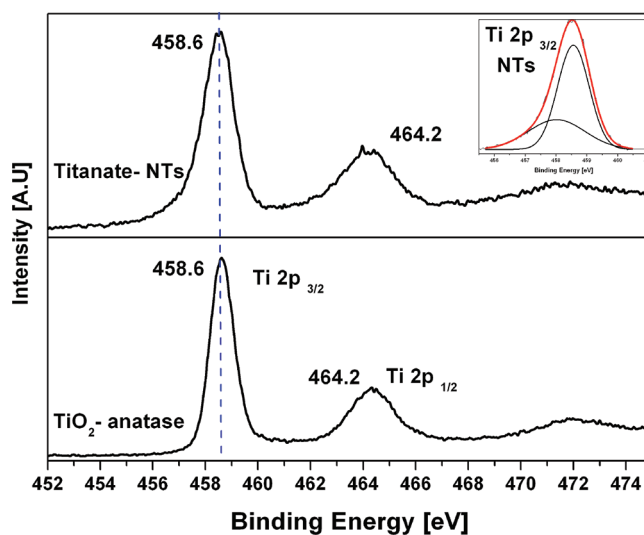


Figure 3. The $Ti\ 2p_{3/2}$ and $Ti\ 2p_{1/2}$ binding energy responses of the treated titanate NTs and the anatase precursor. A small shoulder is observed on the $Ti\ 2p_{3/2}$ peak.

(ESCA) probe with a monochromatic $Al\ K\alpha$ X-ray source, with data collected using Omnicron EIS software. Samples were pressed onto carbon tape held on the sample holder and loaded into the vacuum chamber (1×10^{-10} Torr) for outgassing overnight. The $Ti\ 2p_{3/2}$ and the $Ti\ 2p_{1/2}$ XPS binding energies for both the black NTs and anatase powder are observed at 458.6 and 464.2 eV, respectively (Figure 3). No shift in the $Ti\ 2p_{3/2}$ or the $Ti\ 2p_{1/2}$ binding energy is observed for the titanate NTs compared with the anatase precursor. These binding energies correspond to a Ti^{4+} oxidation state and indicate that the majority of the titanate NTs have a bonding environment similar to that of the original anatase precursor. A small shoulder is observed on the $Ti\ 2p_{3/2}$ peak. To rule out carbon contamination, the intensity of the carbon 1s peak was compared between the two samples. No shift or significant change in intensity for the carbon 1s binding energy resulting from adventitious carbon is observed.¹²

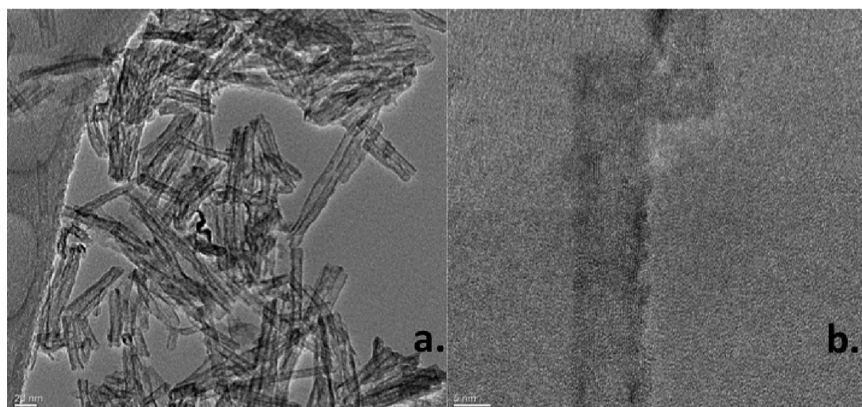


Figure 4. TEM images of titanate nanotube after 5% H₂/Ar treatment in the stainless steel cell. Scaled at (a) 20 and (b) 5 nm.

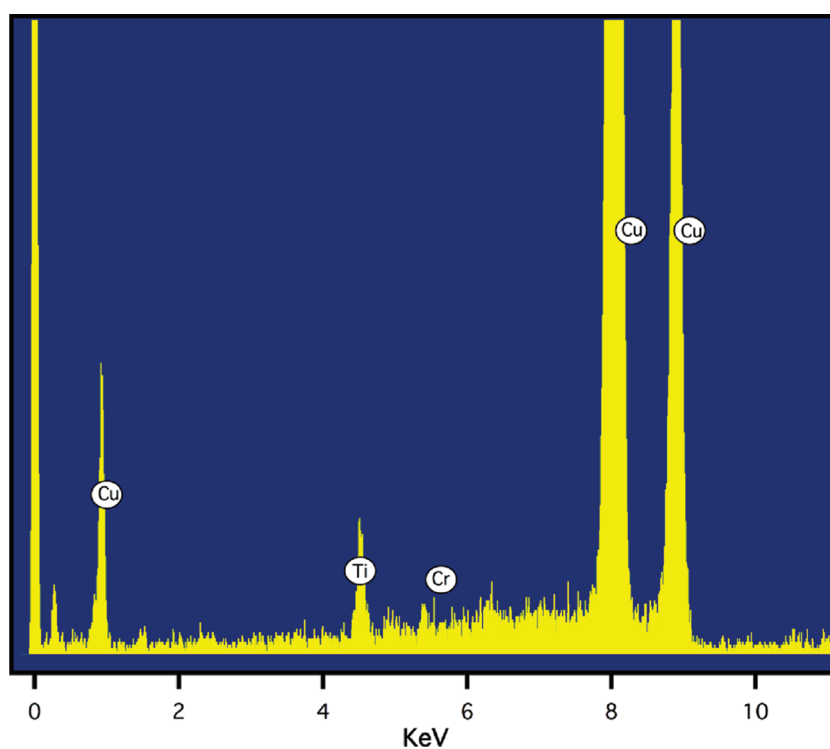


Figure 5. EDS taken of the titanate NTs after being exposed to a flowing atmosphere of 5% H₂/Ar in the stainless steel cell. A small Cr response is observed.

Figure 4 displays TEM images of the NTs after the H₂ treatment in the stainless steel cell and demonstrates that the structural morphology of the titanate NTs remains intact after exposure to H₂ in the cell. This is in agreement with reports that the nanotube 1D morphology collapses only at significantly higher temperatures, ~500 °C.¹⁴ In addition, the TEM images reveal that the inner and outer diameters of the titanate NTs are ~4–6 and 8–12 nm, respectively. In these images, the titanate NTs appear to have asymmetric walls, typically with five layers on one side and three layers on the other, believed to form by scrolling conjoined multilayer nanosheets.¹⁵ TEM images reveal that the difference in the DRUV-vis spectrum of the NTs does not correlate with a change in the morphology of the nanotubes.

Energy-dispersive X-ray spectroscopy (EDS) results taken while performing TEM reveal the presence of Cr in the titanate

nanotubes prepared in the stainless steel reactor (Figure 5). In addition to EDS, an X Series ICP-MS (Thermo Scientific), in CCT mode to negate the ArC interferences, was used to quantify the ⁵²Cr concentration. For sample preparation, the post-H₂-treated titanate NTs were dissolved in an autoclave using concentrated HCl. Three calibration standards and a blank were used to create a standard calibration curve. The ICP-MS experiments were performed in duplicate, and the average Cr concentration is reported. Chromium concentration in the titanate NTs samples prepared in the stainless steel reactor in the presence of hydrogen was found to be ~12 μmol/g H₂Ti₃O₇.

To establish that the choice of reactor material played a role in the properties of the resulting NTs, we carried out the same experiments in a quartz-tube flow reactor at 350 °C under a 5% H₂/Ar flow at atmospheric pressure. After 2 h in the reactor,

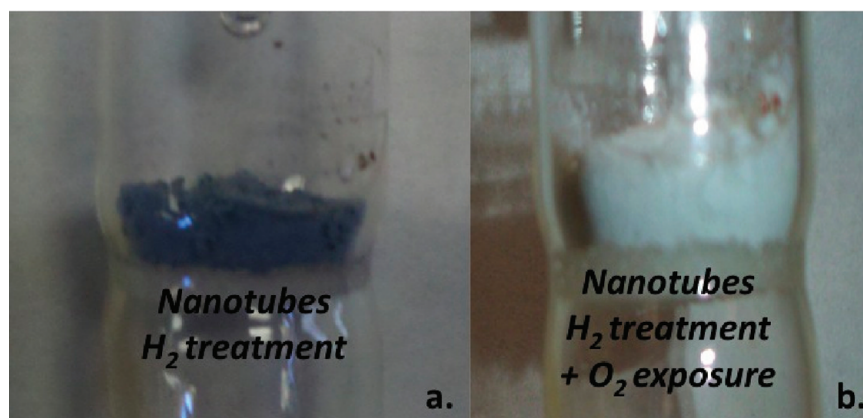


Figure 6. The nanotubes in the quartz reactor after treatment at 350 °C under a flowing atmosphere of 5% H₂ in Ar in a quartz reactor (a) cooled to RT and before exposure to air and (b) after exposure to air (O₂).

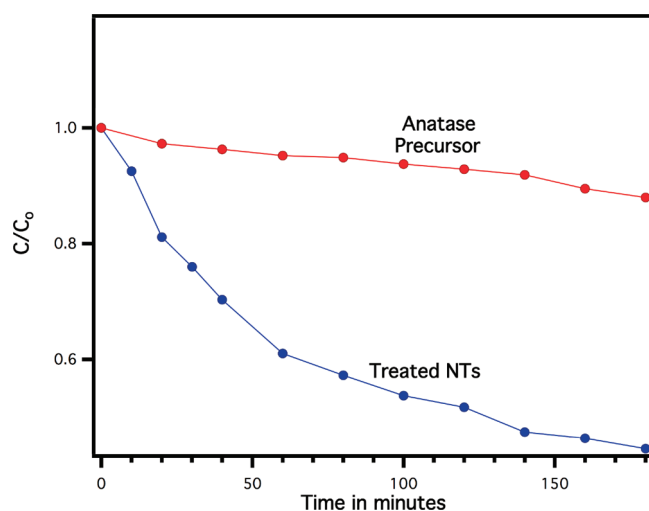


Figure 7. Plot of decrease in concentration of acetaldehyde using visible light in the presence of the treated titanate.

the NTs appear dark blue in color (Figure 6a). This change in color is indicative of oxygen vacancy formation,¹⁹ suggesting that hydrogen readily reacts with surface oxygen to produce, most likely, a combination of water and oxygen vacancies. Upon exposure of the NTs to air, the oxygen vacancies created in the NTs are filled, and a subsequent color change from dark blue to white takes place within a few seconds (Figure 6b). ICP–MS experiments performed on the NTs exposed to hydrogen in the quartz reactor did not show any evidence for the presence of Cr.

The visible light induced photoactivity of the nanotubes treated in hydrogen in the stainless steel reactor, and the anatase precursor powder was studied by following the photodegradation of acetaldehyde. Ten milligrams of either powder was placed in a photocatalytic reactor, described elsewhere,¹⁴ consisting of a closed square Teflon container having a quartz window. One milliliter of saturated acetaldehyde vapor was introduced into the closed chamber and allowed to equilibrate in the dark for 1 h. Photocatalytic reactions were carried out with a xenon arc lamp having an intensity of ~ 55 W/m² and equipped with a long-pass filter to remove wavelengths shorter than 450 nm. As the photocatalytic reaction proceeded, the degradation of acetaldehyde was monitored using an HP 5890 gas chromatograph

equipped with a flame ionization detector (GC-FID). The data in Figure 7 demonstrate the increased photocatalytic activity of the treated titanate NTs compared with anatase powder and confirms that visible light can initiate a photochemical reaction with these NTs. The nonreduced NTs have also been shown to be photocatalytically active for acetaldehyde degradation using UV light.¹⁴

A substantially more pronounced color change that is stable to air exposure is observed for NTs treated in hydrogen using a stainless steel reactor as compared with a quartz tube reactor. This difference in the optical properties of the NTs is attributed to the presence of Cr, which originates in the stainless steel reactor, rather than to changes in the oxidation state of Ti by hydrogenation in the NT material, as was reported in another study.¹² Cr constitutes 11–18% of the total metal content in stainless steel. Yet, under ambient conditions, the surface of stainless steel is coated with a passivating Cr oxide layer that is up to 3 nm thick.¹⁶ A plausible mechanism for Cr transport from the stainless steel to the NTs involves hydrogen embrittlement, a well-known phenomenon for stainless steel and other alloys. Published TEM images taken after exposure of stainless steel to hydrogen reveal that small microvoids (<1 μ m diameter) of low spatial density are produced on the surface of the stainless steel.¹⁷ We hypothesized that the detached particles that produce these microvoids, which are enriched in chromium oxide, are carried to the NTs by the gas flow in the reactor.

We also considered the possible formation of a volatile Cr complex by reaction with hydrogen. Such a complex could be transferred to the sample via the gas flow. However, although a multiplicity of Cr hydride complexes have been identified and characterized, they are unstable at room temperature.^{18,19} Furthermore, even if these complexes form, they are unlikely to be present in significant steady state concentrations under our reaction conditions. Since Cr is found, there may be other metal contaminants in lower quantities originating from the stainless steel reactor, such as iron, carbon, and nickel. However, the concentration of Cr is probably enhanced in the NTs because of the aforementioned surface layer of chromium oxide that forms on stainless steel.

Cr is reported to have a remarkable effect on the electronic structure of titanium oxide materials. Anpo et al. have reported that using a metal ion implantation method, significant changes to the electronic band structure of TiO₂ materials can occur with

Cr loadings as low as $0.6 \mu\text{mol/g}$ of TiO_2 .²⁰ These changes in the electronic band structure were accompanied by a change in reported spectrum that indicated a color change from white to dark gray or black. As indicated previously, XPS experiments performed in our lab comparing the black NTs with the anatase precursor demonstrated little to no difference in the oxidation state of the Ti after air exposure. Thus, we do not see evidence for hydrogenation of the NTs, since incorporation of hydrogen atoms into the surface layers would most likely lead to an observable change in the binding energies of the Ti $2p_{3/2}$ and the Ti $2p_{1/2}$ orbitals. However, as alluded to above, we observe a small shoulder on the Ti $2p_{3/2}$ peak. The shoulder has been observed in a similar system and was assigned to the interaction of Cr with Ti.²¹ The interaction of surface hydroxyls with Ti has also been reported to lead to a shoulder.²¹

In conclusion, we report on the synthesis of titanium oxide NTs and the effect reactor materials can have on the properties of NTs. We verified that the synthesis of the NTs in a stainless steel reactor led to a change in color from white to black, which did not take place under the same conditions in a quartz flow tube reactor. This color change is consistent with the finding that the NTs synthesized in the metal reactor contained Cr. In the quartz tube reactor, an initial change in color from white to blue took place when the NTs were exposed to hydrogen at elevated temperatures. This color change is a result of the formation of oxygen vacancies.²¹ However, unlike the NTs synthesized in the stainless steel reactor, for which the black color persisted, the blue color reverted back to white when the blue NTs were exposed to atmospheric oxygen. No Cr was found in the NTs synthesized in the quartz reactor. The presence of Cr can lead to a major change in the properties of the synthesized materials. These results demonstrate that subtleties in the synthesis of materials can have a profound effect on the properties of materials. In addition, our results demonstrate what appears to be a previously unrealized potential complication involved in the use of metal reactors, particularly for high-temperature syntheses under a hydrogen atmosphere. These conditions appear to be compatible with the transference of Cr from the surface of the reactor, probably in the form of small chromium oxide particles, to the synthesized material, with resultant contamination of the material by Cr.

AUTHOR INFORMATION

Present Addresses

[†]Centre for Materials for Electronics Technology (C-MET), Nano Materials Division, Kerala, India

AUTHOR INFORMATION

[‡]Department of Anthropology, Northwestern University, 1810 Hinman Avenue, Evanston, IL 60208

REFERENCES

- (1) Patzke, G. R.; Krumeich, F.; Nesper, R. *Angew. Chem., Int. Ed.* **2002**, *41*, 2446.
- (2) Mor, G. K.; Shankar, K.; Paulose, M.; Varghese, O. K.; Grimes, C. A. *Nano Lett.* **2005**, *5*, 191.
- (3) Vijayan, B. K.; Dimitrijevic, N. M.; Wu, J. S.; Gray, K. A. *J. Phys. Chem. C* **2010**, *114*, 21262.
- (4) Adachi, M.; Murata, Y.; Okada, I.; Yoshikawa, S. *J. Electrochem. Soc.* **2003**, *150*, G488.
- (5) Varghese, O. K.; Gong, D. W.; Paulose, M.; Ong, K. G.; Dickey, E. C.; Grimes, C. A. *Adv. Mater.* **2003**, *15*, 624.

- (6) Paulose, M.; Varghese, O. K.; Mor, G. K.; Grimes, C. A.; Ong, K. G. *Nanotechnology* **2006**, *17*, 398.
- (7) Zhang, H.; Li, G. R.; An, L. P.; Yan, T. Y.; Gao, X. P.; Zhu, H. Y. *J. Phys. Chem. C* **2007**, *111*, 6143.
- (8) Ghicov, A.; Macak, J. M.; Tsuchiya, H.; Kunze, J.; Haeublein, V.; Frey, L.; Schmuki, P. *Nano Lett.* **2006**, *6*, 1080.
- (9) Varghese, O. K.; Paulose, M.; LaTempa, T. J.; Grimes, C. A. *Nano Lett.* **2009**, *9*, 731.
- (10) Dong, F.; Zhao, W. R.; Wu, Z. B. *Nanotechnology* **2008**, *19*, 365607.
- (11) Xiao, Q.; Ouyang, L. L. *J. Phys. Chem. Solids* **2011**, *72*, 39.
- (12) Chen, X.; Liu, L.; Yu, P. Y.; Mao, S. S. *Science* **2011**, *331*, 746.
- (13) Chen, Q.; Zhou, W. Z.; Du, G. H.; Peng, L. M. *Adv. Mater.* **2002**, *14*, 1208.
- (14) Vijayan, B.; Dimitrijevic, N. M.; Rajh, T.; Gray, K. J. *J. Phys. Chem. C* **2010**, *114*, 12994.
- (15) Bavykin, D. V.; Parmon, V. N.; Lapkin, A. A.; Walsh, F. C. *J. Mater. Chem.* **2004**, *14*, 3370.
- (16) Olsson, C. O. A.; Landolt, D. *Electrochim. Acta* **2003**, *48*, 1093.
- (17) Herms, E.; Olive, J. M.; Puiggali, M. *Mater. Sci. Eng., A* **1999**, *272*, 279.
- (18) Wells, J. R.; House, P. G.; Weitz, E. *J. Phys. Chem.* **1994**, *98*, 8343.
- (19) Wang, X. F.; Andrews, L. *J. Phys. Chem. A* **2003**, *107*, 570.
- (20) Anpo, M.; Takeuchi, M. *J. Catal.* **2003**, *216*, 505.
- (21) Diebold, U. *Surf. Sci. Rep.* **2003**, *48*, 53.